RSC Advances

ROYAL SOCIETY OF CHEMISTRY

www.rsc.org/advances

RSC Advances

RSCPublishing

ARTICLE

Bifurcated hydrogen bonding mediated planar 9,10-anthraquinone dyes: synthesis, structure and property†

Cite this: DOI: 10.1039/x0xx00000x

Yong Yang,*[a] Qiao-Xia Wu[a] and Min Xue[b]

Received 00th January 2012,
Accepted 00th January 2012

DOI: 10.1039/x0xx00000x

www.rsc.org/

Abstract: By acylation of mono- and diamino-9,10-anthraquinones with *o*-alkoxylbenzene carbonyl chloride or *o*-alkoxylnaphthalene carbonyl chloride, a series of planar 9,10-anthraquinone dyes were designed and synthesized. Because of formation of bifurcated hydrogen bonds, these dyes adopted planar conformation, which was exemplified by the crystal structure of one dye. The UV-vis absorption spectra and FL (fluorescence) spectra of the dyes were also recorded. The extent of acylation and positions of the amino and/or amide groups substantially affected the dyes' property.

Introduction

Anthraquinones dyes are the second largest class of textile pigments besides carcinogenic azo dyes[1-3]. They are widely used for the coloration of cotton and cellulose fibers as well as for synthetic materials such as polyamides[4-7]. Among which, anthraquinones with amino and hydroxyl substituents gained special attention due to their photochemical and radiation chemical activities[8,9], and also due to their wide pharmacological and biochemical applications[10]. Amino groups present on the 1-, 4-, 5-, 8-positions of 9,10-anthraquinone dyes can form S(6) type[11-13] hydrogen bonds with the quinone oxygen atoms[14-16] (Figure 1, left), which is a good hydrogen bond acceptor. But amino NH_2 is not a good hydrogen bond donor and the hydrogen bond is not strong enough to control the conformation of the whole molecule. We envisioned that if these amino groups are acylated to become amide groups, NHs of the amide groups are good hydrogen bond donors and the hydrogen bonding interaction will become stronger[17-19]. Further more, if another hydrogen bond acceptor is properly located as illustrated in Figure 1, another S(6) type hydrogen bond will form between NH and the ether oxygen atom. Thus an amide NH contacts with two hydrogen bond donors to form a bifurcated hydrogen bond[20,21] (Figure 1, right). The high strength of this bifurcated hydrogen bond will control the whole molecule to be planar. The anthraquinone motif will form a large conjugated system with the terminal benzene or naphthalene motifs by virtue of successive S(6) type hydrogen bonds. The successful control of conformation will lead to special absorption and emission properties.

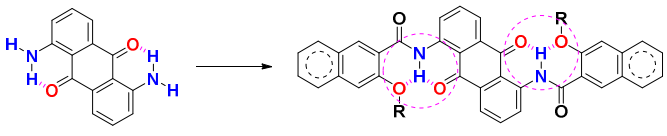

Fig. 1 From amino-anthraquinone to amide-anthraquinone, with bifurcated hydrogen bonding highlighted.

In this article, we describe the synthesis of ten planar 9,10-anthraquinone dyes with bifurcated hydrogen bonding controlling their conformation. A 2-substituted dye that does not incorporate a bifurcated hydrogen bond was also synthesized as control compound. X-Ray single crystal structure analysis of one of the dyes confirmed its planar conformation. Absorption and fluorescence emission spectra for 15 dyes (including four commercially available dyes) were recorded.

Experiment section

The syntheses of the target dyes were straight forward as outlined in Scheme 1~3. The corresponding carboxylic acids with an alkoxyl group presenting at the *ortho* position were first converted to their acyl chlorides upon refluxing in thionyl chloride, and then the acyl chlorides reacted directly with amino-derived anthraquinones in the presentence of triethylamine as base to give the target compounds. Because of strong electron withdrawing ability of the quinone oxygen atoms, the electron density of the amino groups is low and the reactivity is greatly reduced. Even over two equivalent acyl chlorides were used for the above coupling reactions, we separated mono-acylated products with diaminoanthraquinones as reagents. As control, dye **15**, where a bifurcated hydrogen bond is not expected, was also synthesized. All the target compounds were thoroughly characterized by ^{1}H NMR, ^{13}C NMR, HRMS, UV-vis and FL spectroscopy.

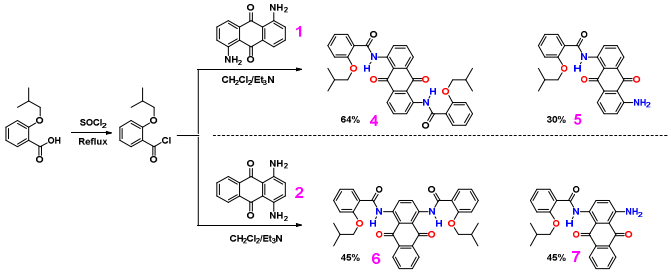

Scheme 1. Synthetic routes for dyes **4**~**7**.

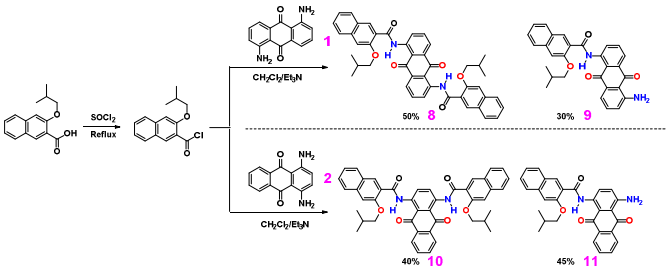

Scheme 2. Synthetic routes for dyes **8**~**11**.

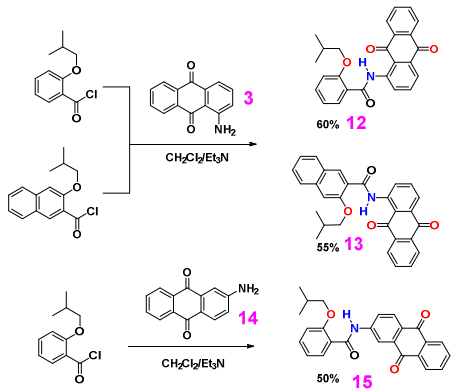

Scheme 3. Synthetic routes for dyes **12**, **13** and **15**.

General procedure for the preparation of acyl chloride

A solution of appropriate carboxylic acid (usually 10 mmol) in 10 mL thionyl chloride was heated under reflux with a calcium chloride drying tube equipped for 8 hours. Then the solvent was removed under reduced pressure. The crude acyl chloride was used directly for the next step without further purification and characterization.

General procedure for acylation

A solution of the above prepared acyl chloride (usually 10 mmol) in CH_2Cl_2 (30 mL) was added into a suspension of 1,5-diaminoanthraquinone (1.19 g, 5 mmol), or 1,4-diaminoanthraquinone (1.19 g, 5 mmol), or 1-aminoanthraquinone (2.23 g, 10 mmol), and triethylamine(2.1 mL, 15 mmol) in CH_2Cl_2 (40 mL) dropwise over a period of 30 minutes with an ice-water bath equipped. After addition, the ice-water bath was removed, and the reaction mixture was heated to reflux. After 9 hours, more CH_2Cl_2 (100 mL) was added. The solution was washed with 2 N diluted HCl (30 mL), saturated Na_2CO_3 aqueous solution (30 mL) and saturated brine (30 mL) successively. The organic layer was dried over anhydrous Na_2SO_4. The solvent was evaporated under reduced pressure. The crude product was subjected to column chromatography. Usually for the diaminoanthraquinones, di- and mono-acylated products were both separated.

Characterization data for dyes

All solvents for reactions and column chromatography were used directly as received. Melting points were uncorrected. ^{1}H and ^{13}C NMR spectra were recorded on a Bruker AV 400 MHz or 300 MHz instruments. Chemical shifts were expressed in parts per million (δ) using residual solvent protons as internal standards. Chloroform (δ = 7.26 ppm) was used as an internal standard for chloroform-*d*. Alcohol free chloroform was used as solvent for spectroscopic measurements, which was thoroughly washed with distilled water and freshly distilled from P_2O_5. UV-vis data were recorded on UV-2501 PC SHIMADZU and the FL measurements in solution on a PerkinElmer Precisely LS45.

Dye **4**:
Yield: 64%; Color: yellow.
Mp: 244-245 °C.
^{1}H NMR (300 MHz, $CDCl_3$, TMS, 298 K, ppm): δ 12.98 (s, 2H, N*H*), 9.32 (d, *J* = 7.9 Hz, 2H, Ar*H*), 8.09-8.01 (m, 4H, Ar*H*), 7.80 (t, *J* = 8.1 Hz, 2H, Ar*H*), 7.50 (td, *J* = 7.5 Hz, *J* = 1.5 Hz,2H, Ar*H*), 7.13-7.04 (m, 4H, Ar*H*), 4.10 (d, *J* = 6.9 Hz, 4H, OCH_2), 2.36-2.20 (m, 2H, C*H*), 0.97 (d, *J* = 6.7 Hz, 12H, CH_3).
^{13}C NMR (75 MHz, $CDCl_3$, TMS, 298 K, ppm): δ 185.6, 166.1, 157.0, 141.5, 135.3, 135.0, 133.2, 132.0, 127.4, 123.7, 122.4, 120.8, 118.4, 112.7, 75.5, 27.7, 19.3.
FT-IR (KBr, cm^{-1}): 3203, 3158, 3115, 2967, 2957, 2924, 2905, 2867, 1665, 1651, 1595, 1576, 1502, 1479, 1469, 1450, 1405, 1339, 1310, 1269, 1027, 753, 706.
MS: *m/z* (EI) 590 (M^+), 414, 238, 177, 121 (100).
Elemental analysis calcd (%) for $C_{36}H_{34}N_2O_6$·½H_2O: C 72.10, H 5.88, N 4.67; found: C 72.35, H 5.88, N 4.71.

Dye **5**:
Yield: 30%; Color: orange.
Mp: 172.3-172.7 °C.
^{1}H NMR (400 MHz, $CDCl_3$, TMS, 298 K, ppm): δ 13.06 (s, 1H, N*H*), 9.26 (d, *J* = 8.5 Hz, 1H, Ar*H*), 8.10 (d, *J* = 7.5 Hz, 1H, Ar*H*), 8.03 (d, *J* = 7.6 Hz, 1H, Ar*H*), 7.80 (t, *J* = 8.0 Hz, 1H, Ar*H*), 7.58 (d, *J* = 7.3 Hz, 1H, Ar*H*), 7.48 (q, *J* = 7.3 Hz, 2H, Ar*H*), 7.08(t, *J* = 7.8 Hz, 2H, Ar*H*), 6.97 (d, *J* = 8.1 Hz, 1H, Ar*H*), 4.06 (d, *J* = 6.8 Hz, 2H, OCH_2), 2.32-2.20 (m, 1H, C*H*), 0.95 (d, *J* = 6.3 Hz, 6H, CH_3).
^{13}C NMR (100 MHz, $CDCl_3$, TMS, 298 K, ppm): δ 186.3, 184.7, 166.1, 157.0, 150.7, 141.4, 135.5, 135.3, 135.1, 134.8, 133.0, 131.9, 126.4, 124.1, 122.7, 122.1, 120.8, 118.8, 117.1, 113.2, 112.7, 75.4, 27.8, 19.3.
MS: *m/z* (EI) 414 (M^+), 238(100), 177, 121.

Dye **6**:
Yield: 40%; Color: orange.
Mp: 177.3-177.9°C.
^{1}H NMR (300 MHz, $CDCl_3$, TMS, 298 K, ppm): δ 13.10 (s, 2H, N*H*), 9.28 (s, 2H, Ar*H*), 8.23(q, *J* = 3.3 Hz, *J* = 2.5 Hz, 2H, Ar*H*), 8.07 (dd, *J* = 8.7 Hz, *J* = 1.8 Hz, 2H, Ar*H*), 7.78 (q, *J* = 3.3 Hz, *J* = 2.5 Hz, 2H, Ar*H*), 7.49 (td, *J* = 8.7 Hz, *J* = 1.8 Hz, 2H, Ar*H*), 7.08 (t+d, *J* = 8.0 Hz, 4H, Ar*H*), 4.08 (d, *J* = 6.9 Hz, 4H, CH_2), 2.37-2.22 (m, 2H, C*H*), 0.98 (d, *J* = 6.7 Hz, 12H, CH_3).
^{13}C NMR (100 MHz, $CDCl_3$, TMS, 298 K, ppm): δ 185.9, 165.9, 157.0, 137.9, 134.1, 133.6, 133.2, 132.1, 130.1, 126.8, 123.6, 120.9, 118.8, 112.6, 75.5, 27.8, 19.3.
HRMS (ESI$^+$) calcd. for $[C_{36}H_{34}N_2O_6+H]^+$ 591.2495, found: 591.2492; calcd. for $[C_{36}H_{34}N_2O_6+Na]^+$ 613.2315, found: 613.2310.

Dye **7**:
Yield: 45%; Color: red.
Mp: 142-143 °C.
^{1}H NMR (400 MHz, $CDCl_3$, TMS, 298 K, ppm): δ 13.09 (s, 1H, N*H*), 9.02 (d, *J* = 9.6 Hz, 1H, Ar*H*), 8.31 (d, *J* = 7.5 Hz, 1H, Ar*H*), 8.23 (d, *J* = 7.4 Hz, 1H, Ar*H*), 8.05 (d, *J* = 7.6 Hz, 1H, Ar*H*), 7.82-7.70 (m, 2H, Ar*H*), 7.48 (t, *J* = 7.9 Hz, 1H, Ar*H*), 7.08 (t, *J* = 8.3 Hz, 3H, Ar*H*), 4.06 (d, *J* = 6.8 Hz, 2H, CH_2), 2.30-2.22 (m, 1H, C*H*), 0.97 (d, *J* = 6.2 Hz, 6H, CH_3).
^{13}C NMR (100 MHz, $CDCl_3$, TMS, 298 K, ppm): δ 185.8, 184.6, 165.8, 157.0, 148.2, 134.2, 134.1, 133.8, 133.7, 133.0, 132.9, 131.8, 131.0, 126.7, 126.5, 125.6, 124.0, 120.8, 118.3, 112.7, 111.5, 75.5, 27.8, 19.3.
HRMS (ESI$^+$) calcd. for $[C_{25}H_{22}N_2O_4+H]^+$ 415.1658, found: 415.1656; calcd. for $[C_{25}H_{22}N_2O_4+Na]^+$ 437.1477, found: 437.1475; calcd. for $[2*C_{25}H_{22}N_2O_4+Na]^+$ 851.3057, found: 851.3055.

Dye **8**:
Yield: 50%; Color: yellow.
Mp: > 300 °C.
^{1}H NMR (400 MHz, $CDCl_3$, TMS, 298 K, ppm): δ 13.08 (s, 2H, N*H*), 9.38 (d, *J* = 8.4 Hz, 2H, Ar*H*), 8.57(s, 2H, Ar*H*), 8.07 (d, *J* = 7.3 Hz, 2H, Ar*H*), 7.91 (d, *J* = 7.9 Hz, 2H, Ar*H*), 7.85(t, *J* = 8.0 Hz, 2H, Ar*H*), 7.79 (d, *J* = 8.0 Hz, 2H, Ar*H*), 7.55 (t, *J* = 7.0 Hz, 2H, Ar*H*), 7.41 (t, *J* = 7.1 Hz, 2H, Ar*H*), 7.34 (s, 2H, Ar*H*), 4.19 (d, *J* = 6.5 Hz, 4H, OCH_2), 2.41-2.29 (m, 2H, C*H*), 1.02 (d, *J* = 6.3 Hz, 12H, CH_3).
^{13}C NMR (100 MHz, $CDCl_3$, TMS, 298 K, ppm): δ 185.7, 166.1, 154.0, 141.4, 136.1, 135.5, 135.0, 133.2, 129.0, 128.4, 128.0, 127.4, 126.4, 125.3, 124.4, 122.6, 118.3, 107.4, 75.4, 27.7, 19.4.
HRMS (ESI$^+$) calcd. for $[C_{44}H_{38}N_2O_6+Na]^+$ 713.2628, found: 713.2629.

Dye **9**:
Yield: 30%; Color: orange.
M.p. 207.4-208.0 °C.
^{1}H NMR (400 MHz, $CDCl_3$, TMS, 298 K, ppm): δ 13.13 (s, 1H, N*H*), 9.32 (d, *J* = 8.2 Hz, 1H, Ar*H*), 8.53 (s, 1H, Ar*H*), 8.12 (d, *J* = 7.3 Hz, 1H, Ar*H*), 7.90 (d, *J* = 7.8 Hz, 1H, Ar*H*), 7.83 (t, *J* = 8.0 Hz, 1H, Ar*H*), 7.77 (d, *J* = 7.9 Hz, 1H, Ar*H*), 7.60-7.50 (m, 2H, Ar*H*), 7.47 (t, *J* = 7.4 Hz, 1H, Ar*H*), 7.40 (t, *J* = 7.1 Hz, 1H, Ar*H*), 7.31 (s, 1H, Ar*H*), 6.98 (d, *J* = 8.0 Hz, 1H, Ar*H*), 4.13 (d, *J* = 6.8 Hz, 2H, CH_2), 2.40-2.25 (m, 1H, C*H*), 0.99 (d, *J* = 6.5 Hz, 6H, CH_3).
^{13}C NMR (100 MHz, $CDCl_3$, TMS, 298 K, ppm): δ 186.4, 184.7, 166.1, 154.0, 150.8, 141.3, 136.0, 135.5, 135.3, 135.2, 134.9, 132.9, 129.0, 128.2, 128.0, 126.3, 125.7, 124.4, 122.8, 122.3, 118.7, 117.2, 113.1, 107.4, 75.3, 27.7, 19.4.
HRMS (ESI$^+$) calcd. for $[C_{29}H_{24}N_2O_4+Na]^+$ 487.1634, found: 487.1632; calcd. for $[2*C_{29}H_{24}N_2O_4+Na]^+$ 951.3370, found: 951.3368.

Dye **10**:
Yield: 40%; Color: orange.
Mp: 178.3-179.3 °C.
^{1}H NMR (400 MHz, $CDCl_3$, TMS, 298 K, ppm): δ 13.23 (s, 2H, N*H*), 9.41 (s, 2H, Ar*H*), 8.62 (s, 2H, Ar*H*), 8.26 (t, *J* = 4.4 Hz, 2H, Ar*H*), 7.93 (d, *J* = 8.2 Hz, 2H, Ar*H*), 7.81 (d, *J* = 8.0 Hz, 4H, Ar*H*), 7.57(t, *J* = 7.6 Hz, 2H, Ar*H*), 7.43 (t, *J* = 7.4 Hz, 2H, Ar*H*), 7.35 (s, 2H, Ar*H*),4.20 (d, *J* = 6.8 Hz, 4H, OCH_2), 2.44-2.33 (m, 2H, C*H*), 1.05 (d, *J* = 6.5 Hz, 12H, CH_3).
^{13}C NMR (100 MHz, $CDCl_3$, TMS, 298 K, ppm): δ 186.0, 165.9, 154.0, 138.0, 136.0, 134.2, 133.6, 133.3, 130.1, 129.1, 128.3, 128.1, 126.9, 126.3, 125.3, 124.4, 118.7, 107.4, 75.4, 27.7, 19.4.
HRMS (ESI$^+$) calcd. for $[C_{44}H_{38}N_2O_6+H]^+$ 691.2808, found: 691.2805; calcd. for $[C_{44}H_{38}N_2O_6+Na]^+$ 713.2628, found: 713.2625.

Dye **11**:
Yield: 45%; Color: red.
Mp: 207.4-208.0 °C.
^{1}H NMR (400 MHz, $CDCl_3$, TMS, 298 K, ppm): δ 13.17 (s, 1H, N*H*), 9.09 (d, *J* = 9.4 Hz, 1H, Ar*H*), 8.54 (s, 1H, Ar*H*), 8.31 (d, *J* = 7.5 Hz, 1H, Ar*H*), 8.23 (d, *J* = 7.5 Hz, 1H, Ar*H*), 7.89 (d, *J* = 8.0 Hz, 1H, Ar*H*), 7.76 (m, 3H, Ar*H*), 7.53 (t, *J* = 7.4 Hz, 1H, ArH), 7.39 (t, *J* = 7.3 Hz, 1H, Ar*H*), 7.30 (s, 1H, Ar*H*), 7.12 (d, *J* = 9.4 Hz, 1H, Ar*H*), 4.14 (d, *J* = 7.0 Hz, 2H, CH_2), 2.42-2.28 (m, 1H, C*H*), 1.00 (d, *J* = 6.6 Hz, 6H, CH_3).
^{13}C NMR (100 MHz, $CDCl_3$, TMS, 298 K, ppm): δ 186.0, 184.6, 165.8, 154.1, 148.2, 135.9, 134.12, 134.09, 133.8, 133.7, 133.1, 132.9, 130.9, 129.0, 128.2, 128.0, 126.7, 126.5, 126.3, 125.8, 125.6, 124.3, 118.2, 111.5, 107.4, 75.4, 27.7, 19.4.
HRMS (ESI$^+$) calcd. for $[C_{29}H_{24}N_2O_4+H]^+$ 465.1814, found: 465.1813; calcd. for $[C_{29}H_{24}N_2O_4+Na]^+$ 487.1634, found: 487.1632; calcd. for $[2*C_{29}H_{24}N_2O_4+Na]^+$ 951.3370, found: 951.3370.

Dye **12**:
Yield: 60%; Color: yellow.
Mp: 190.8-191.3 °C.
^{1}H NMR (400 MHz, $CDCl_3$, TMS, 298 K, ppm): δ 13.02 (s, 1H, N*H*), 9.33 (d, *J* = 8.5 Hz, 1H, Ar*H*), 8.32-8.24 (m, 2H, Ar*H*), 8.12 (d, *J* = 7.8 Hz, 1H, Ar*H*), 8.05 (d, *J* = 8.0 Hz, 1H, Ar*H*), 7.82 (t+d, *J* = 7.7 Hz, 3H, Ar*H*), 7.50 (t, *J* = 8.2 Hz, 1H, Ar*H*), 7.09 (t, *J* = 6.9 Hz, 2H, Ar*H*), 4.09 (d, *J* = 6.5 Hz, 2H, CH_2), 2.32-2.22 (m, 1H, C*H*), 0.97 (d, *J* = 6.8 Hz, 6H, CH_3).
^{13}C NMR (100 MHz, $CDCl_3$, TMS, 298 K, ppm): δ 186.0, 183.0, 166.1, 157.0, 141.7, 135.3, 134.3, 134.2, 134.17, 134.10, 133.2, 132.8, 132.0, 127.7, 127.2, 127.0, 123.7, 122.7, 120.9, 118.9, 112.7, 75.4, 27.8, 19.3.
HRMS (ESI$^+$) calcd. for $[C_{25}H_{21}NO_4+H]^+$ 400.1549, found: 400.1547; calcd. for $[C_{25}H_{21}NO_4+Na]^+$ 422.1368, found: 422.1364; calcd. for $[2*C_{25}H_{21}NO_4+Na]^+$ 821.2839, found: 821.2840.

Dye **13**:
Yield: 55%; Color: yellow.
Mp: 179.8-180.1 °C.
^{1}H NMR (400 MHz, $CDCl_3$, TMS, 298 K, ppm): δ 13.12 (s, 1H, N*H*), 9.41 (d, *J* = 8.5 Hz, 1H, Ar*H*), 8.57 (s, 1H, Ar*H*), 8.33 (t, *J* = 4.4 Hz, 1H, Ar*H*), 8.29 (t, *J* = 4.3 Hz, 1H, Ar*H*), 8.17 (d, *J* = 7.5 Hz, 1H, Ar*H*), 7.93 (d, *J* = 8.2 Hz, 1H, Ar*H*), 7.88 (t, *J* = 8.3 Hz, 1H, Ar*H*), 7.85-7.78 (m, 3H, Ar*H*), 7.57 (t, *J* = 7.7 Hz, 1H, Ar*H*), 7.43 (t, *J* = 7.5 Hz, 1H, Ar*H*), 7.35 (s, 1H, Ar*H*), 4.19 (d, *J* = 7.0 Hz, 2H, CH_2), 2.41-2.29 (m, 1H, C*H*), 1.03 (d, *J* = 6.5 Hz, 6H, CH_3).
^{13}C NMR (100 MHz, $CDCl_3$, TMS, 298 K, ppm): δ 186.1, 183.0, 166.0, 153.9, 141.7, 136.0, 135.4, 134.3, 134.2, 134.14, 134.10, 133.1, 132.8, 129.0, 128.3, 128.0, 127.5, 127.2, 127.0, 126.3, 125.4, 124.4, 122.8, 118.8, 107.4, 75.3, 27.7, 19.4.
HRMS (ESI$^+$) calcd. for $[C_{29}H_{23}NO_4+H]^+$ 450.1705, found: 450.1704; calcd. for $[C_{29}H_{23}NO_4+Na]^+$ 472.1525, found: 472.1523; calcd. for $[2*C_{29}H_{23}NO_4+Na]^+$ 921.3152, found: 921.3152.

Dye **15**:
Yield: 50%; Color: yellow.
Mp: 188.1-188.5 °C.
^{1}H NMR (400 MHz, $CDCl_3$, TMS, 298 K, ppm): δ 10.52 (s, 1H, N*H*), 8.50 (d, *J* = 7.6 Hz, 1H, Ar*H*), 8.37-8.29 (m, 4H, Ar*H*), 8.24 (s, 1H, Ar*H*), 7.80(t, *J* = 3.8 Hz, 2H, Ar*H*), 7.54 (t, *J* = 7.0 Hz, 1H, Ar*H*), 7.16 (t, *J* = 7.7 Hz, 1H, Ar*H*), 7.06 (d, *J* = 8.2 Hz, 1H, Ar*H*), 4.05 (d, *J* = 6.5 Hz, 2H, CH_2), 2.45-2.35 (m, 1H, C*H*), 1.22 (d, *J* = 6.7 Hz, 6H, CH_3).
^{13}C NMR (100 MHz, $CDCl_3$, TMS, 298 K, ppm): δ 182.9, 182.1, 163.8, 157.0, 144.1, 134.7, 134.2, 134.0, 133.8, 133.7, 133.6, 132.7, 129.4, 129.0, 127.2, 127.1, 124.8, 121.7, 120.8, 117.0, 112.5, 76.0, 28.6, 19.5.

Results and discussion

^{1}H NMR analysis

^{1}H NMR study (Figure 2, see supporting information Figure S1 for ^{1}H NMR spectra of dyes **8**, **9**, **10**, **11** and **13**) in chloroform first confirmed the formation of bifurcated hydrogen bonds. Very sharp signals for amide N*H*s, irrespective of mono-acylated or di-acylated dyes, all appeared at a very downfield region, δ > 13 ppm. Furthermore little changes were observed for the ^{1}H NMR spectra in a wide range of concentrations (from 50 mM to 0.5 mM). While the signal for NH in compound **15**, where bifurcated hydrogen bonding

is not available, appeared at 10.52 ppm. The very downfield chemical shift of NH must result from strong bifurcated intramolecular hydrogen bonding interactions.

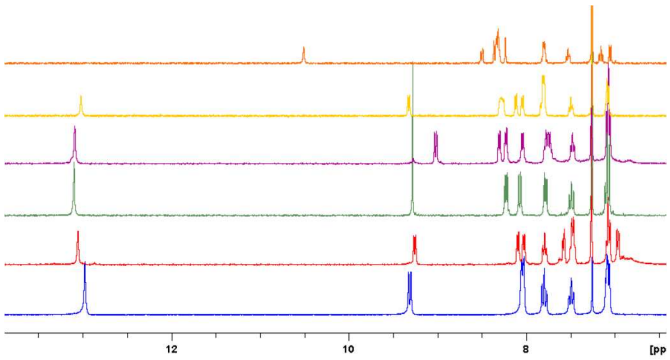

Fig. 2 Stacked partial ^{1}H NMR spectra of dyes **4**, **5**, **6**, **7**, **12** and **15**, from bottom up, $CDCl_3$, 400 MHz, 298 K.

X-Ray single crystal analysis

Direct evidence for the bifurcated hydrogen bonding came from X-Ray single crystal analysis of dye **4** (Figure 3). By slow evaporation of a solution of compound **4** in dichloromethane and methanol, we obtained a needle-like single crystal suitable for X-Ray analysis[22]. As expected, by incorporating two *iso*-butyloxy groups into the molecule, four highly favorable S(6) type hydrogen-bonded rings formed. Distances between O (*iso*-butyloxy) and H (amide), O (anthraquinone carbonyl oxygen) and H (amide), O (*iso*-butyloxy) and O(anthraquinone carbonyl oxygen) are 2.009 Å, 2.001 Å, 2.802 Å respectively, which are much shorter than the sums of van der Waals radii of O and H (2.7 Å, 26% shorter), O and O (3.04 Å, 7.8% shorter). The angles of O (isobutyloxy oxygen)···H—N and the O (anthraquinone carbonyl oxygen)···H—N are 135.53° and 132.94° respectively. Because of these strong bifurcated hydrogen bonds, the molecule resides its framework almost at a plane. The dihedral angle between ring A and ring B is just 14.3°. Ring A and ring C are parallel to each other. This planar conformation facilitated its further π-π interaction with other molecules. As illustrated in Figure 4 typic off-set π-π stacking mode[23] is observed. An interlayer distance (vertical displacement) is 3.43 Å, which is substantially smaller than the sum of the van der Waals radii of two sp^2 carbon atoms and is comparable to the interlayer distance in graphite (3.4 Å). The horizontal displacement is 3.7 Å. Overall, one third of the anthraquinone ring overlaps. This arrangement can bring about the maximum stacking energy[24].

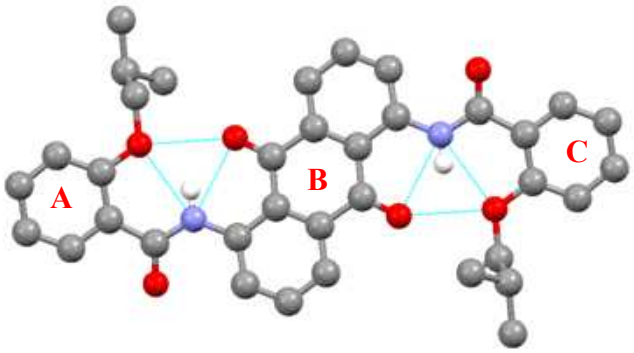

Fig. 3 Crystal structure (ball and stick model) of dye **4**. All hydrogen atoms except NHs were omitted for clarity. Due to the strong S(6) type hydrogen-bonds, the molecule was predefined to be planar and formed a large conjugated system.

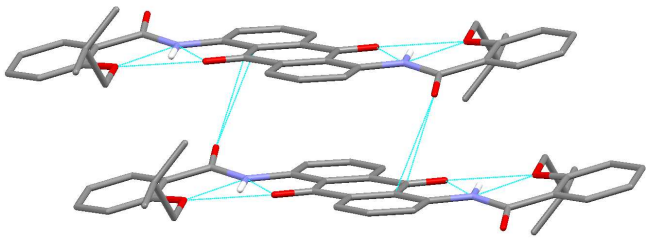

Fig. 4 Illustration of π-π stacking mode in solid state (capped sticks model). For clarity, all hydrogen atoms except N*H*s were omitted.

UV-vis and FL studies

Upon acylation the dyes displayed different colours. The extent of acylation and the positions of amino and/or amide groups are the two main factors determining the colours. Pictures for each dye in dilute chloroform solution were summarized in Figure 5. The colours range from red to purple. UV-vis absorption and fluorescence emission spectra for each dye were summarized in Figure 6~8 and Table 1.

Fig. 5 Photos for dyes (from left to right) **1-15**, 5×10^{-5} M in chloroform solution.

Table 1. Absorption and emission maxima for dyes.

	1	**4**	**5**	**8**	**9**	**2**	**6**	**7**
Absorption maxima (nm)[a]	476	437	466	438	470	544 581	479	523
Emission maxima (nm)[b]	538	514	548	511	548	604	569	596
ε (10^4 L·mol^{-1}·cm^{-1})	1.41	1.36	1.17	1.61	1.36	0.94	0.88	0.83
	10	**11**	**3**	**12**	**13**	**14**	**15**	
Absorption maxima (nm)[a]	480	523	463	416	416	409	378	
Emission maxima (nm)[b]	568	596	541	512	509	523	521	
ε (10^4 L·mol^{-1}·cm^{-1})	0.82	1.32	0.72	0.63	0.82	0.18	0.47	

[a] Only absorption maxima in the visible region; [b] λ_{ex} = 430 nm.

For dyes with 1,5-substituted anthraquinone cores (**1**, **4**, **5**, **8** and **9**, Figure 6), the acylation of amino groups leads to hypsochromic shift of absorption maxima in the visible light region. For un-acylated dye **1**, the absorption maximum is at 476 nm; for mono-acylated dyes **5** and **9**, 466 nm and 470 nm are observed respectively; for di-acylated dyes **4** and **8**, 437 nm and 438 nm are observed respectively. The terminal groups, benzene or naphthalene,

do not affect the absorption spectra substantially. But the terminal groups affect the fluorescence emission intensity substantially. Un-acylated dye **1** shows an emission band at 538 nm. For mono-acylated **5** and **9**, the emission maxima are both at 548 nm with almost the same intensity. While for di-acylated **4** and **8**, the emission maxima are at 514 nm and 511 nm respectively, and the intensity for the former is larger than the later.

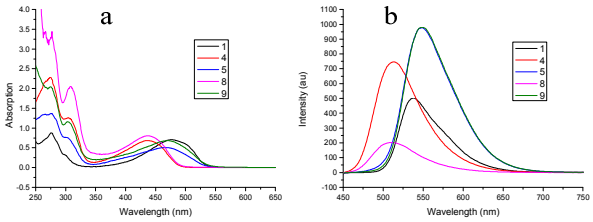

Fig. 6 (a) UV-vis spectra for dyes **1**, **4**, **5**, **8** and **9**, 5×10^{-5} M in chloroform; (b) Fluoresence emission spectra for dyes **1**, **4**, **5**, **8** and **9**, 1×10^{-5} M in chloroform, λ_{ex} = 430 nm.

For dyes with 1,4-substituted anthraquinone cores (**2**, **6**, **7**, **10** and **11**, Figure 7), similar trend was observed for absorption spectra: the absorption maxima in the visible light region showed hypsochromic shift upon acylation, from 544 nm and 581 nm (dye **2**, un-acylated) to 523 nm (**7** and **11**, mono-acylated) to 480 nm (**6** and **10**, di-acylated). But conditions are quite different for fluorescence behavior. The un-acylated **2** is almost non-emissive when excited with 430 nm. The mono-acylated products **7** and **11** show moderate emission. Greatly enhanced emission is observed for the di-acylated products **6** and **10**.

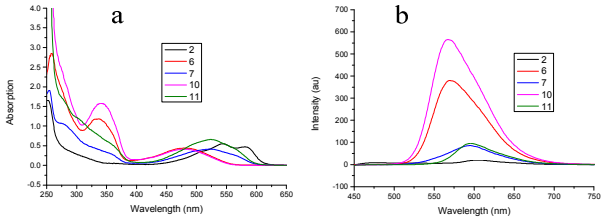

Fig. 7 (a) UV-vis spectra for dyes **2**, **6**, **7**, **10** and **11**, 5×10^{-5} M in chloroform; (b) Fluoresence emission spectra for dyes **2**, **6**, **7**, **10** and **11**, 1×10^{-5} M in chloroform, λ_{ex} = 430 nm.

For the third type of dyes with 1-substituted anthraquinone cores (**3**, **12** and **13**, Figure 8), the absorption follows the above mentioned trend: acylation leads to hypsochromic shift. Dye **14** and **15** are almost UV-vis transparent: very weak absorption are observed. But the fluorescence behavior runs out of the above framework: compared with 1-amino-9,10-anthraquinone **3**, the emission is substantially quenched when acylation with *o*-alkoxynaphthalene carbonyl chloride (dye **13**) and a little enhanced with *o*-alkoxybenzene carbonyl chloride (dye **12**). Dye **14** with an amino group at position 2 shows very strong emission intensity, but acylation of the amino group leads to almost completely quenching of the fluorescence (dye **15**).

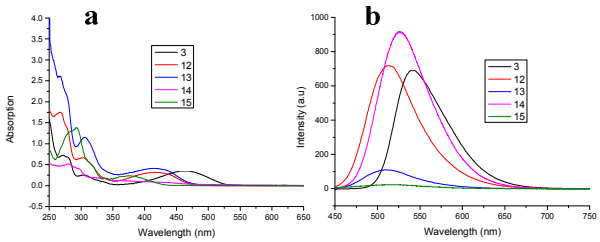

Fig. 8 (a) UV-vis spectra for dyes **3**, **12**, **13**, **14** and **15**, 5×10^{-5} M in chloroform; (b) Fluoresence emission spectra for dyes**3**, **12**, **13**, **14** and **15**, 1×10^{-5} M in chloroform, λ_{ex} = 430 nm.

Conclusions

In summary, we introduced bifurcated hydrogen bonding strategy to mediate planar conformation of 9,10-anthraquinone dyes by acylation of amino groups at 1-, 4-, and 5-positions. ^{1}H NMR and X-Ray single crystal analysis confirmed the success of our strategy. After acylation of the amino groups the whole dye molecule adopts planar conformation and becomes a large conjugated system, which substantially reduces the energy of the π orbit. Thus the maximum absorption wavelength, which corresponds to π-π* transition, shows hypsochromic shift. Furthermore, the extent of acylation and the positions of functional groups also substantially affect the spectroscopic property of dyes. This strategy of bifurcated hydrogen bonding will bring about new idea and platform for the design and synthesis of new anthraquinone dyes.

Acknowledgements

This work was supported by the Program for Zhejiang Leading Team of Science and Technology Innovation (No. 2010R50038-18), Zhejiang Natural Science Foundation (Grant LY12B02021) and 521 talent program of Zhejiang Sci-Tech University.

Notes and references

[a] Department of Chemistry, Key Laboratory of Advanced Textile Materials and Manufacturing Technology of Education Ministry, Zhejiang Sci-Tech University, Hangzhou 310018, China.
Email: yangyong@zstu.edu.cn. Tel: (+86)-571-86843228
[b] Department of Physics, Zhejiang Sci-Tech University, Hangzhou 310018, China.
† Electronic Supplementary Information (ESI) available: [NMR spectra for all dyes and CIF for the single crystal of dye **4**]. See DOI: 10.1039/b000000x/

1 J.R. Aspland. *Textile Dyeing and Coloration*. American Association of Chemists and Colorists: Research Triangle Park, NC, USA, 1997; pp 251.
2 R. E. Kirk and D. F. Othmer, Eds. *Dyes*. In *Encyclopedia of Chemical Technology*. Wiley: Hoboken, NJ, 2005; Vol. 9, pp 300–347.
3 A. K. Mishra, J. Jacob and K. Müllen, *Dyes Pigm.*, 2007, **75**, 1-10.
4 J. S. Manson and D. R. A. Ridyard. *Anthraquinone Dyes*. U.S. Patent 3935248, Jan 27, 1976.
5 E. Marechal, *Prog. Org. Coat.*, 1982, **10**, 251-287.
6 J. Miley, Pure Appl. Chem., 1996, **68**, 1423–1428.
7 C. Dollendorf, S. K. Kreth, S. W. Choi and H. Ritter, *Beilstein J. Org. Chem.*, 2013, **9**, 453-459.
8 T. Yatsuhashi and H. Inoue, *J. Phys. Chem. A*, 1997, **101**, 8166-8173.
9 J. P. Rasimas and G. J. Blanchard, *J. Phys. Chem.*, 1995, **99**, 11333-11338.

10 Y. Duan, J. Yu, S. Liu and M. Ji, *Med. Chem.*, 2009, **5**, 577-582.
11 M. C. Etter, *Acc. Chem. Res.*, 1990, **23**, 120-126.
12 M. C. Etter, J. C. MacDonald and J. Bernstein, *Acta Crystallogr. Sect. B*, 1990, **46**, 256-262.
13 J. Bernstein, R. E. Davis, L. Shimoni and N.-L. Chang, *Angew. Chem., Int. Ed. Engl.*, 1995, **34**, 1555-1573.
14 P. Dahiya, D. K. Maity, S. K. Nayak, T. Mukherjee and H. Pal, *J. Photochem. Photobiol. A*, 2007, **186**, 218-228.
15 P. Dahiya, M. Kumbhakar, T. Mukherjee and H. Pal, *J. Mol. Struct.*, 2006, **798**, 40-48.
16 P. Dahiya, M. Kumbhakar, D. K. Maity, T. Mukherjee, A. B. R. Tripathi, N. Chattopadhyay and H. Pal, *J. Photochem. Photobiol. A*, 2006, **181**, 338-347.
17 F. H. Beijer, R. P. Sijbesma, J. A. J. M. Vekemans, E. W. Meijer, H. Kooijman and A. L. Spek, *J. Org. Chem*., 1996, **61**, 6371-6380.
18 H.-Y. Hu, J.-F. Xiang, J. Cao and C.-F. Chen, *Org. Lett.*, 2008, **10**, 5035-5038.
19 H.-Y. Hu, J.-F. Xiang and C.-F. Chen, *Org. Biomol. Chem.*, 2009, **7**, 2534-2539.
20 Z.-Q. Wu, X.-K. Jiang, S.-Z. Zhu and Z.-T. Li, *Org. Lett.*, 2004, **6**, 229-232.
21 R. D. Parra, H. Q. Zeng, J. Zhu, C. Zheng, X. C. Zeng and B. Gong, *Chem. Eur. J.*, 2001, **7**, 4352-4357.
22 Crystal data: $C_{36}H_{34}N_2O_6$, M_w = 590.65, crystal size: 0.79×0.15×0.13 mm^3, crystal system: monoclinic, space group P2(1)/n, a = 5.1550(10), b = 23.851(5), c =11.944(2) Å, β = 93.18(3)°, U = 1466.3(5) $Å^3$, Z = 2, D_c = 1.338 Mg/m^3, T = 293(2) K, μ(Mo-K_α) = 0.71073 mm^{-1}, 11881 reflections measured, 3297 unique (R_{int} = 0.0623), R_1 = 0.0506, wR_2 =0.1091. The data was deposited in the Cambridge Crystallographic Data Centre (CCDC) with the reference No 250831. These data can be obtained free of charge via www.ccdc.cam.ac.uk.
23 C. A. Hunter and J. K. M. Sanders, *J. Am. Chem. Soc.*, 1990, **112**, 5525-5534.
24 S. Toyota, M. Goichi and M. Kotani, *Angew. Chem. Int. Ed.*, 2004, **43**, 2248-2251.

